water

MDPI

Article

Inundation Analysis of Reservoir Flood Based on Computer Aided Design (CAD) and Digital Elevation Model (DEM)

Jiqing Li, Jianchang Li * and Kaiwen Yao

Renewable Energy School, North China Electric Power University, Beijing 102206, China; jqli6688@163.com (J.L.); kwyao@ncepu.edu.cn (K.Y.)

* Correspondence: lijianchang08@outlook.com; Tel.: +86-156-5075-9350

Received: 23 February 2018; Accepted: 16 April 2018; Published: 23 April 2018

Abstract: GIS (Geographic Information System) can be used to combine multiple hydrologic data and geographic data for FIA (Flood Impact Assessment). For a developing country like China, a lot of geographic data is in the CAD (Computer Aided Design) format. The commonly used method for converting CAD into DEM may result in data loss. This paper introduces a solution for the conversion between CAD data and DEM data. The method has been applied to the FIA based on the topographic map of CAD in Hanjiang River. When compared with the other method, the new method solves the data loss problem. Besides, the paper use GIS to simulate the inundation range, area, and the depth distribution of flood backwater. Based on the analysis, the author concludes: (1) the differences of the inundation areas between the flood of HQ_{100} and the flood of HQ_{50} are small. (2) The inundation depth shows a decreasing trend along the upstream of the river. (3) The inundation area less than 4 m in flood of HQ_{50} is larger than that in flood of HQ_{100}, the result is opposite when the inundation depth is greater than 4 m. (4) The flood loss is 392.32 million RMB for flood of HQ_{50} and 610.02 million RMB for flood of HQ_{100}. The method can be applied to FIA.

Keywords: Geographic Information System (GIS); CAD; DEM

1. Introduction

Due to the characteristics of operation, the standard of resettlement for water project may be other criteria. There are still a large amount of land, population, and houses that are above the relocation scope. When the reservoirs encounter rare floods, backwater level of flood controlled will increase to a higher level than natural floods, and so does the time of flood. It will lead to the inundation in the reservoir area, which will cause loss and affect production and the life of the residents around the reservoir. Establishing flood simulation system can help to handle emergencies, and reduce the risk and loss of life and property [1]. Therefore, it is necessary to do the flood impact assessment in order to minimize the loss of inundation. Then, the government can make appropriate measures to protect the legitimate rights of the people in the reservoir area and to promote social stability and economic development in the reservoir area [2–4].

Geographic Information System (GIS) has a strong capability of spatial analysis. It can obtain more analysis results and more accurate results by combining multiple hydrologic data and geographic data for Flood Impact Assessment (FIA). Some researchers used GIS to analyze the different methods of flood inundation under two different conditions, in which the flood water level and volume was given, respectively. Their studies visualized three-dimensional (3D) terrain by ERDAS Virtual GIS and Open GL software packages. They realized the virtual reality expression of inundation zone by ArcGIS Engine based on DEM (Digital Elevation Model) [5]. Besides, GIS is used to develop a flood risk map.

It always combines remote sensing data to make the result of FIA more accurate [6–8]. The models that are used to analyze the urban flood are developed by GIS, such as the GIS-based model for urban flood inundation (GUFIM) and the urban storm flood inundation simulation method (USISM) [9,10]. GIS can analyze the factors that have a greater impact on urban floods, combined with Analytical Hierarchy Process (AHP) and multi-criteria decision analysis (MCDA) [11,12]. Lyu [13] analyzed the relationship between flood risk and urbanization. The author concluded that one of the significant influential factors of flooding was identified as the urbanization degree. In order to improve the drainage capacity and reduce the harm of urban floods, Daniel [14] designed a site selection methodology for the location prioritization of PPS (Permeable Pavement Systems) in urban catchments. Some researchers used SAR (Synthetic Aperture Radar), TM (Thematic Mapper), and GIS data to extract the floodplain of the coastal plain. Their studies compared the hydrodynamic models and GIS for coastal flood vulnerability assessment (CFVA). The results indicated that hydrodynamic models are more appropriate for detailed CFVA, but GIS can be used for FIA in large areas [15,16]. It can be seen that GIS plays an important role in FIA. However, GIS is based on geographic information data, such as DEM. Bhuyian [17] found that NED-based (National Elevation Dataset based) hydrodynamic modeling resulted in a high overestimation of the simulated flood stage, but the SRTM-based (Shuttle Radar Topography Mission based) model was unable to produce any reasonable result prior to DEM correction. Error in simulated flood consequence dropped following the DEM correction. Walczak et al. [18] compared four DEMs that were based on various data sources (SRTM, ASTER GDEM (Advanced Spaceborne Thermal Emission and Reflection Radiometer Global Digital Elevation Model), LIDAR (light detection and ranging), and aerial photographs) to calculate the polder retention capacity. The authors concluded that the accuracy of ASTER or SRTM DEMs is generally insufficient for flood modeling, especially for modelling polders' capacity as flood-protection systems. The same authors emphasized that, in the absence of a high resolution DEM based on LIDAR data, the DEM that was developed on the basis of aerial photographs can be used after some correction based on field measurements. Saksena and Merwade [19] have analyzed the impact of DEM resolution and accuracy on the flood inundation mapping. They pointed out that water surface elevations (WSE) along the stream and the flood inundation area are in a linear relationship with both DEM resolution and accuracy. Sande [20] compared the coastal flood risk assessment using various publicly available DEMs and LIDAR DEMs. The author concluded that the publicly available DEMs do not meet the accuracy requirement of coastal flood risk assessments, especially in coastal and deltaic areas. Heimhuber [21] combined a 12 m spatial resolution TanDEM-X (a German radar satellite) digital elevation model (DEM) and a 30 cm spatial resolution DEM created with mapping drones. The study obtained more accurate results of river flood simulation. Ireneusz [22] presented a method for the correction of low quality DEMs, which was based on aerial photographs. The analyses indicated that, after the correction procedure, the predictions of corrected DEM based on poor quality data is in good quantitative and qualitative agreement with the referenced LIDAR DEM. Amir [23] introduced the Height Above Nearest Drainage (HAND) method in his study, and the model is more suitable for the analysis of storm flood inundation. For a developing country like China, a lot of geographic information data is in the CAD (Computer Aided Design) format. How to use the data available is worth studying. The US National Park Service [24] proposed the requirements for the conversion between CAD and GIS. Besides, it provided guidance for the conversion. Rebecca [25] applied the CAD system's "b-rep" design to extend the two-dimensional (2D) surface information to the 3D direction based on the manifold model. But his study was limited in the extension of the TIN model. Pu [26] proposed that CAD systems have many different shapes, but the shapes are limited to point, line, and polygon features for GIS. The author suggested that DBMS (Data Base Management System) plays an intermediary role in data conversion. DBMS can provide the missing data types and make the system access the data that it can understand. The method ensured the consistency of data at the DBMS level. Zlatanova [27] considered that adopting DBMS scheme in CAD and GIS system storage model design is a good choice for data conversion between CAD and GIS. However, this scheme is more complicated and requires higher professionalism of operators.

Ratchata [28] discussed the possibility of semantic interoperability between CAD and GIS. The author proposed an ontology engineering method to solve the semantic differences problem of CAD and GIS data query. The method requires strong professional knowledge to write procedures, which is not conducive to the promotion. Jelena [29] created a model to implement CAD-to-GIS transformation by ModelBuilder in GIS. However, the method has high requirements on CAD data, and it is not convenient for the handling of non-standard CAD data.

At present, the commonly used method for converting CAD into DEM is like this: Firstly, the elevation data is exported as a table (EXCEL or database table). Then, the table is imported into GIS. Finally, the data is converted to DEM in GIS. However, some elevation points are attribute blocks in CAD. The blocks cannot be exported to the table, resulting in data loss. What is more, because the EXCEL table has a limited number of rows, the data may be exported incompletely. In order to solve the problems above, this paper applied a solution for the conversion between CAD data and DEM data. The method is applied to the FIA based on the topographic map of CAD in Hanjiang area. When compared with the general method, the scheme solves the data loss problem.

Due to the impoundment of the Gaobei Hydropower Project, the flood backwater level is higher than the nature flood. It is necessary to analyze the flood impaction. The paper used GIS to simulate the inundation range, area, and the depth distribution of flood backwater. In addition, the inundation loss is estimated based on physical indicators (Figure 1 for flowchart to simulate the inundation range). The information of the flood inundation can be obtained timely, accurately, and systematically, providing a scientific basis for flood losses evaluation and making a flood risk distribution map. As well as, it provides support for government departments to make flood control decisions and to guide the local residents to arrange production.

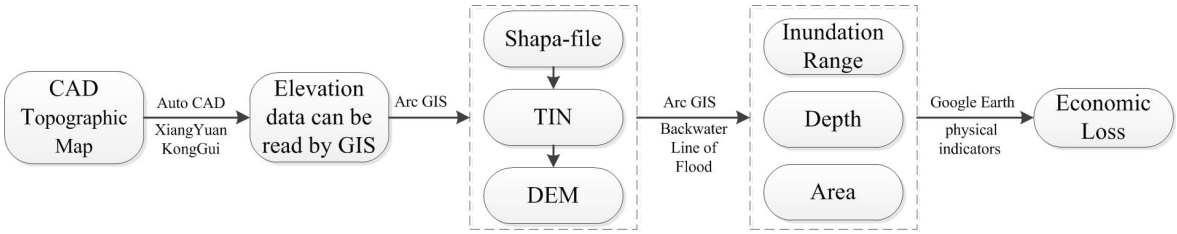

Figure 1. The flowchart to simulate the inundation range.

2. Methods

2.1. Data Conversion

The method of converting CAD to DEM can be described as follow: (1) Use the command "EXPLODATT" to spilt the attribute blocks of CAD into the point and the elevation value in XiangYuanKongGui (This is a software made by a Chinese organization); (2) Import the CAD data to GIS; (3) Extract the elevation data into the Shape-file in GIS; (4) Check and correct the error data of the Shape-file; (5) Convert the Shape-file to TIN; and, (6) Convert the TIN to the DEM of raster.

2.1.1. Import CAD into GIS

At present, topographic maps and other geographic information data of China are mainly the DWG format data of CAD. How to apply the CAD data to the GIS is a critical issue. In general, the conversion between the different data formats can be divided into direct conversion and indirect conversion. Direct conversion refers to reading and writing data directly between two different systems, which is more efficient, but it is necessary to know the data structure of the two systems. Due to commercial reasons, the data structure of most professional software is not disclosed; direct conversion cannot be used in most cases. Indirect conversion refers to the reading data between two different systems through intermediate data. Most commercial software defines an exchange file,

usually ASCII files, such as DXF data of Auto CAD. However, due to the lack of uniform description of spatial objects, the original data information cannot be expressed completely and accurately after the conversion, resulting in some information loss. Moreover, the user must know the details of the exchange format and data format of application system, the programming skills, and workload requirements of users are high.

ESRI provides a solution for using and sharing CAD data. The data exchange between the ArcGIS and CAD system usually has three kinds of technical methods, namely file conversion, direct access, and sharing interface of database [30], as shown in Figure 2, CAD/GIS direct access is to use CAD data as a GIS dataset to read CAD drawings directly from local files. Arc GIS can access many CAD formats directly, including DWG format of Auto CAD, ASCII files, and DXF files of binary.

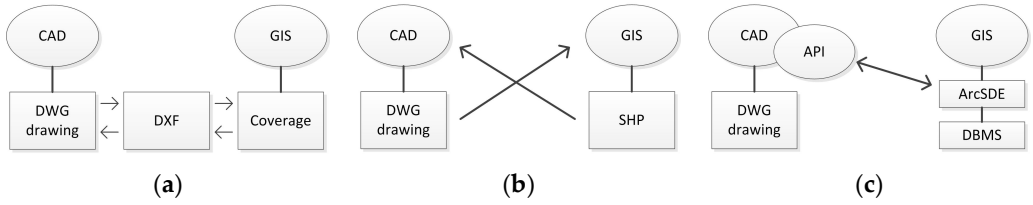

Figure 2. Three kinds methods of CAD (Computer Aided Design) data to Geographic Information System (GIS). (**a**) Description of file conversion; (**b**) Description of direct access; and, (**c**) Description of sharing interface of database.

Actually, GIS can convert data between different types of files, including CAD and DEM files. For example, DXF data of topographic mapping, JPEG images, TIFF files with spatial coordinate information, ESRI Shape-files data, MapInfo TAB data, web PNG data, SVG data, and GeoJson data, et al. GDAL/OGR is a class library for geospatial data conversion. It is used to read geospatial data. According to the data on the GDAL official website, GDAL/OGR supports up to 132 kinds of raster data and 71 types of vector data.

2.1.2. Using CAD to Generate DEM

Using CAD data to establish DEM requires elevation points of CAD with elevation properties. As shown in Figure 3, the attribute block with an elevation point and annotation of elevation value. GIS cannot identify the attribute blocks. The block will be recognized as a polygon in GIS. Before importing CAD data to GIS, command "EXPLODATT" must be used to split the attribute blocks into elevation points and the elevation value annotation in XianYuanKongGui. Then, the data can be read by the GIS.

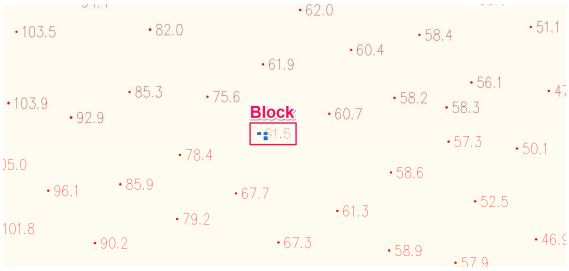

Figure 3. Schematic diagram of elevation points in CAD.

(1) Extraction of CAD elevation data

Topographic map of CAD includes a variety of layers superimposed. Layer of elevation point is generally named GCD in CAD, but the elevation data belong to the layer named Annotation in

ArcGIS. The elevation data can be extracted as a Shape-file by the "Analysis-Extract-Select" tool in ArcToolbox, as shown in the Figure 4a.The accuracy of DEM will directly affect the accuracy of the FIA results [31,32]. The data imported in the above manner usually has some problems. In particular, some of the elevation values are not precise and they will cause errors in the generated TIN file. Therefore, we need to use Field Calculator in the Attribute Table to correct the elevation data based on the data of the Text field, Figure 4b.

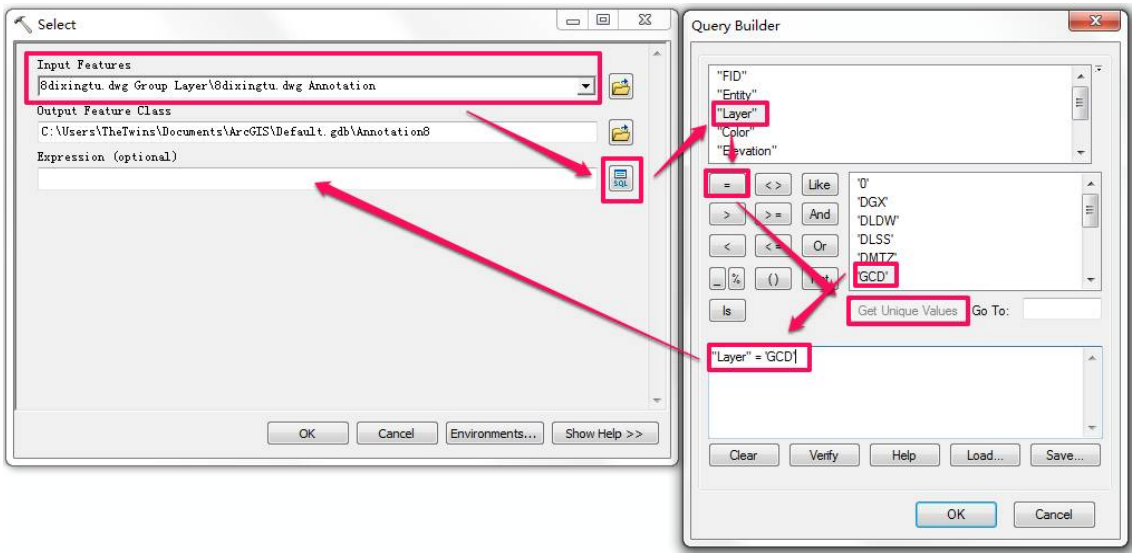

(**a**)

	Elevation	RefName	Style	Text
1	0	83.3	HZ	83.3
1	0	82.9	HZ	82.9
1	0	82.8	HZ	82.8
1	0	77.9	HZ	77.9
1	0	84.4	HZ	84.4
1	0	77.4	HZ	77.4
1	0	78.1	HZ	78.1
1	0	82.6	HZ	82.6
1	0	79.4	HZ	79.4
1	0	74.3	HZ	74.3
1	0	78.8	HZ	78.8
1	0	84.7	HZ	84.7
1	0	83.6	HZ	83.6
1	0	78.7	HZ	78.7
1	0	80.2	HZ	80.2
1	0	80.8	HZ	80.8
1	30.24	30	HZ	30
1	30.24	2	HZ	2
1	30.69	30	HZ	30
1	30.69	7	HZ	7
1	30.69	30	HZ	30
1	30.69	7	HZ	7
1	30.86	30	HZ	30
1	30.86	9	HZ	9
1	30.86	30	HZ	30
1	30.86	9	HZ	9
1	31.15	31	HZ	31
1	31.15	2	HZ	2

(**b**)

Figure 4. Elevation data extracted by the "Analysis-Extract-Select" tool in ArcToolbox (**a**) Produce to extract the elevation data; and, (**b**) The text field in the attribute table.

(2) Convert CAD elevation data to DEM

The elevation point of CAD is a vector file, but GIS cannot convert the vector elevation points into the continuous planar raster DEM. Therefore, the paper converts the elevation points to TIN by interpolation, and converts the TIN into a raster DEM file. We firstly use the "3D Analyst Tools—Data Management—TIN—Create TIN" tool in ArcToolbox to create TIN. Then, we use the "3D Analyst Tools—Conversion—From TIN—TIN to Raster" tool in ArcToolbox to convert the TIN file to DEM. Finally, we get the DEM file, as shown in Figure 5.

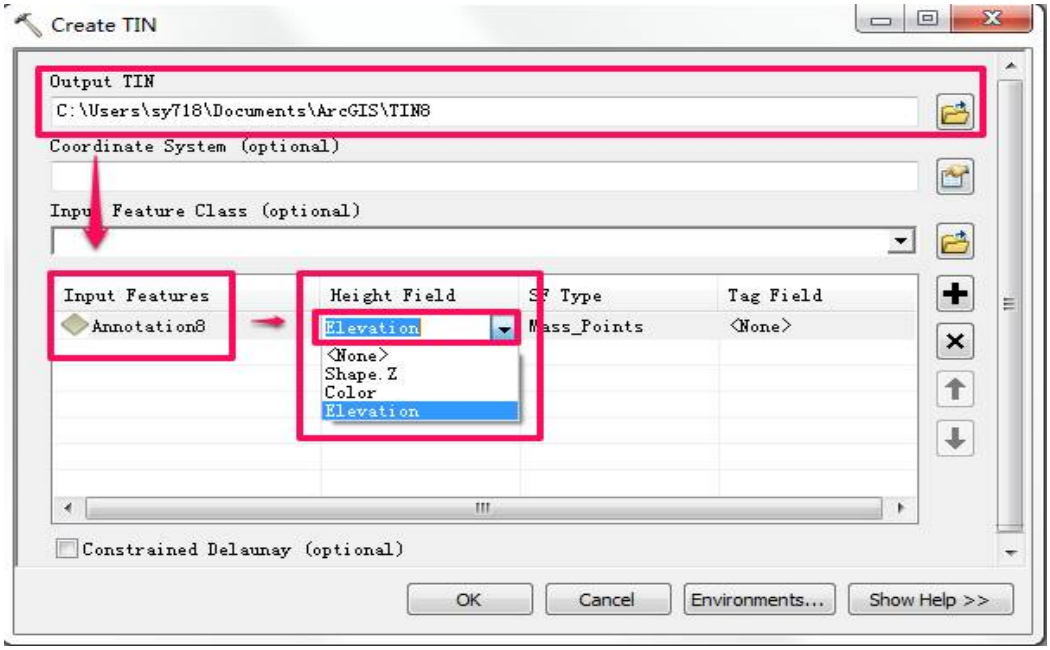

(**a**)

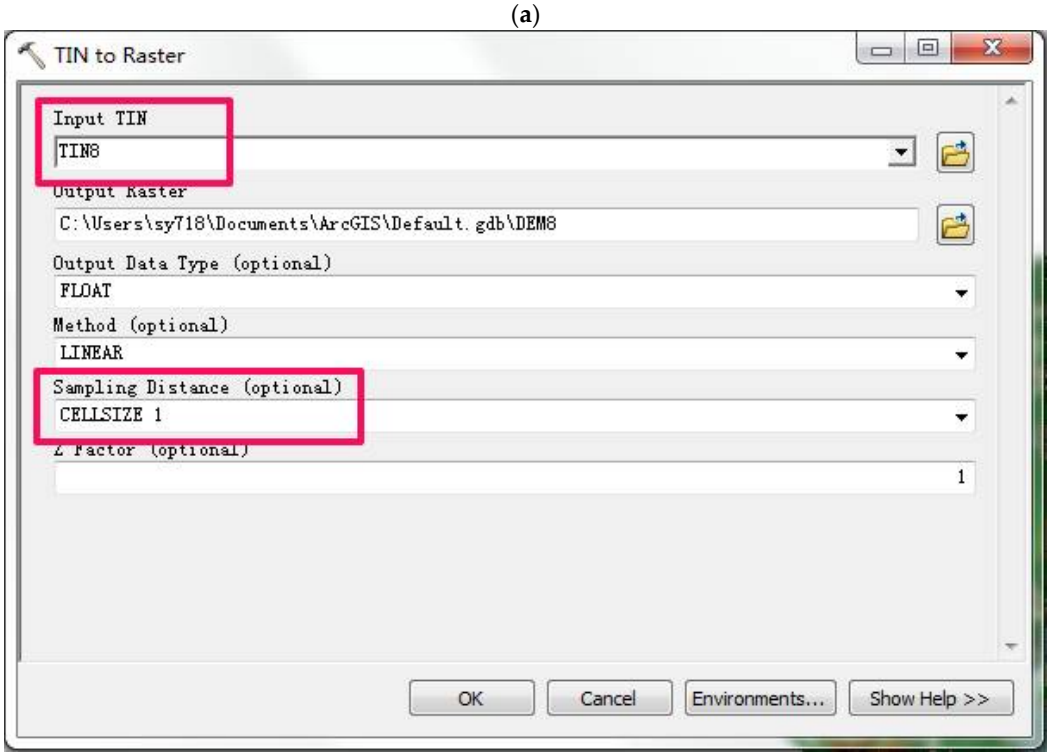

(**b**)

Figure 5. *Cont.*

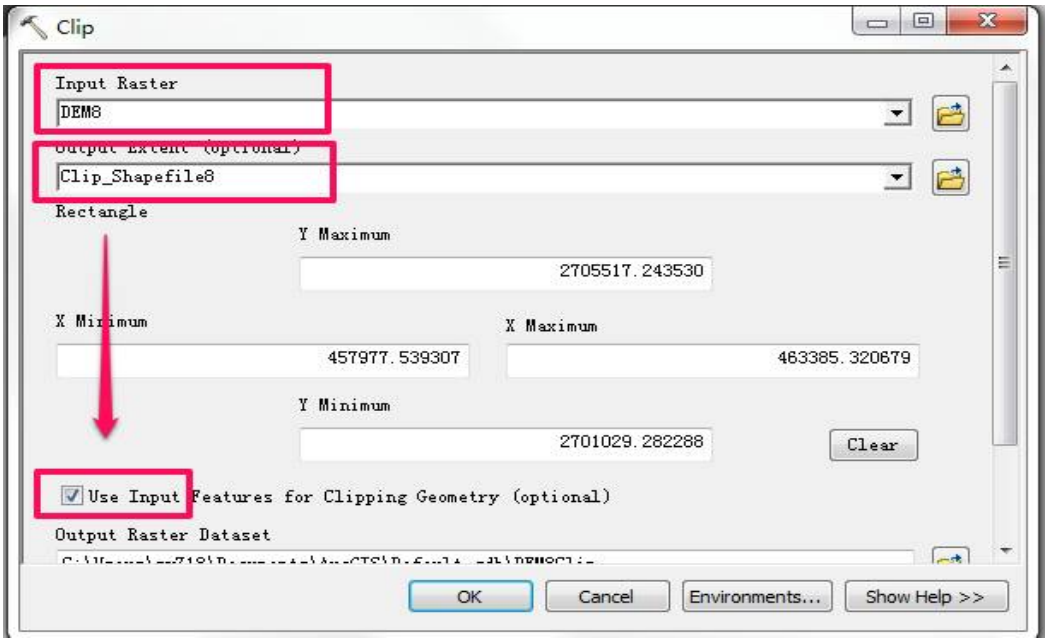

(**c**)

Figure 5. Produce to convert Shape-file to digital elevation model (DEM). (**a**) Creating TIN from Shape-file; and, (**b**) Creating DEM from TIN; and, (**c**) Clipping DEM to obtain that we needed.

2.2. Flood Inundation Analysis Based on DEM

The most commonly used algorithm for FIA is the seed inundation algorithm. The core of this method is to give certain physical properties (such as water level) to the seed points and to spread the water flow in four or eight directions within the plane area until the boundary [33,34]. The seed inundation algorithm can be divided into non-source flooding and source flooding, depending on whether connectivity is considered or not [35–37].

Non-source flooding refers to the point of which the elevation below a given water level is recorded as the inundation area. The condition is similar to that the entire area has uniform precipitation and all low-lying areas may be flooded. Because it does not involve regional connectivity, depression merger, surface runoff, and other complex issues, the analysis is relatively simple. In this situation, inundation depth is considered relative with rainfall at a certain extent. Non-source flooding analysis is usually used in the flat area, of which terrain structure is relatively simple. The method does not consider the connectivity between regions. As long as the elevation value of an area is lower than the inundation elevation value, it will be considered as the inundation area. Non-source flooding is relatively easy to realize on the computer. This method is used to determine the inundation of each grid unit given the flood backwater level in this paper.

Source flooding can be divided into flooding with embankment bursting and flooding with embankment overtopping [38]. The former has only one inundation starting point, a starting seed point in other words. This algorithm needs to consider the directionality of the water flow. According to the characteristics of the water flow, the water will only flow in one of the eight directions with the highest elevation difference. It is suitable for river flood simulation. The latter has more than one inundation starting points. This algorithm does not need to consider the directionality of the water flow. That is, the water will flow in all directions of eight directions below the seed point. It is more suitable for the simulation of lake flood inundation.

3. Study Area and Materials

3.1. Study Area

Hanjiang River is one of the most important rivers in the southeast of China. The Hanjiang River basin covers a drainage area of 30,112 square kilometers. The upper reaches of the Hanjiang River are merged by Meijiang and Tingjiang. The total length of the main stream is 470 km. Both sides of the river are populated areas. There are mountains on the outside of the populated areas. When flood occurs, flood spreads to the river bank, but flood is limited between the mountains on both sides of the river.

The Gaobei Hydropower Project, located in Dapu County, Guangdong Province, China, is a large-scale water control project on the Hanjiang River (Figure 6). The main tasks of the project are flood control, water supply, and power generation and shipping. When the reservoirs encounter floods of HQ_{100} or HQ_{50}, the backwater level after flood control is higher than that of the natural flood waters with the same return period. The time of flooding will be extended and so as the flooding losses to the periphery of the reservoir. In order to reduce flood hazards, analyzing the FIA of Hangjiang River is necessary.

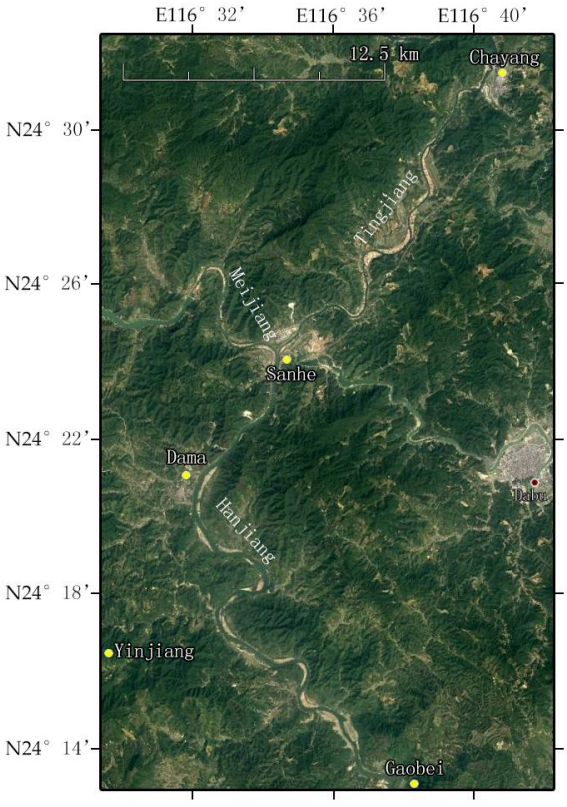

Figure 6. The schematic diagram of study area.

3.2. Materials

(1) Backwater line of flood. When the flood of HQ_{50} or HQ_{100} occurs, the water level of former in the reservoir is 44.67 m and the latter is 47.44 m. The backwater affected areas are: section from Meijiang to Penglatan Power Station with 9.15 km away from Meijiang River estuary and 38.62 km away from the dam site; section from Tingjiang to Chayang Power Station with 25.65 km away from Tingjiang estuary and 55.13 km away from dam site.

The backwater data is obtained from Guangdong Hydropower Planning & Design Institute (a comprehensive investigation and design institute in China). According to the national regulations of

China, backwater is calculated using the Bernoulli equation. The dam site is used as the initial section to calculate the backwater along upstream, using the Bernoulli equation between two adjacent sections. When the level difference between the backwater and the natural water is 0.1–0.3 m (the end of the backwater), the calculation stops. Backwater is corrected according to the height of wave run-up and ship wave run-up.

(2) Topographic map of CAD. Topographic map of CAD includes the section from the dam site to the town of Sanher in Hanjiang, section from Sanhe town to the Penglatan Power Station in Meijiang and section from Sanhe town to Chayang Power Station in Tingjiang, and sides of the river. Topographic data covers the range that is affected by the flood basically.

3.3. Data Processing

(1) Generation of DEM. Firstly, import the CAD file after splitting the blocks in XiangYuanKongGui into ArcGIS. Secondly, extract the elevation data to the Shape-file and correct the error of elevation (Figure 7a, only part of the data). Then, convert the Shape-file to TIN. Finally, convert the TIN file into a raster DEM file. FIA of Hanjing River will be based on the DEM file that is shown in Figure 7b (only partial data).

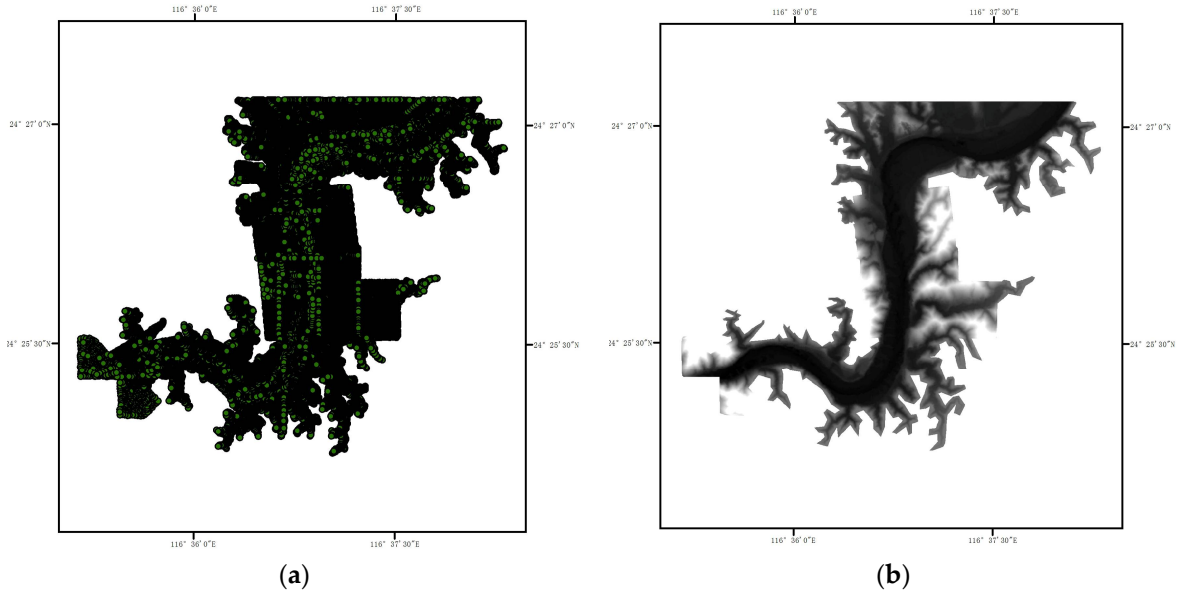

Figure 7. The process of elevation points to DEM. (**a**) The shape-file of elevation points; and, (**b**) The DEM file of raster obtained form (**a**).

(2) Input the section data. Backwater line of flood is section location of the river and the corresponding water level. Section data needs to be established for backwater flooding analysis. Based on the distance between each section and dam site, we measured the distance along the centerline of the main channel and calibrated the cross section position in ArcGIS, as shown in Figure 8. At the same time, the backwater levels at each section are recorded.

(3) Divide the study area according to sections. The method of non-source flooding is used to analyze the flooding of reservoirs, so the area of which elevation is below the return water level are seen as inundation. The average backwater level is used as the basis for determining the inundation area. The study area is divided into several sub-areas, according to the section distribution.

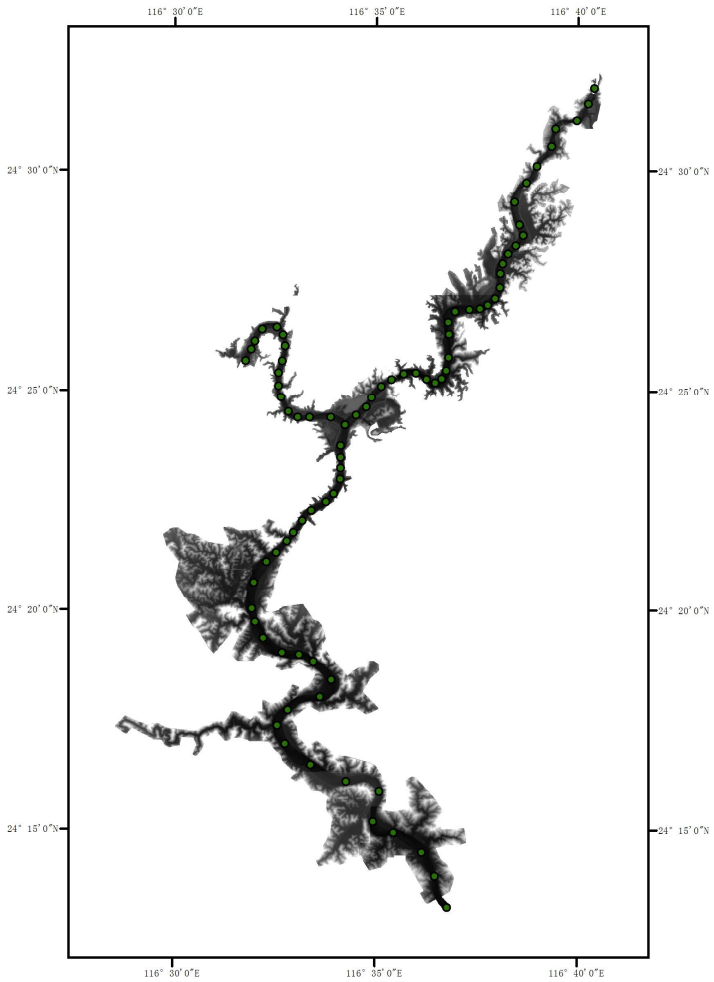

Figure 8. Different sections of backwater (marked by green points).

4. Results and Disscussion

4.1. Analysis of Inundation Range of Study Area

According to the corresponding average backwater water level, the raster calculator tool is used to extract the area below the backwater level as the inundation area for each divided sub-area. With the DEM and the survey, the inundation range can be corrected. After that, the inundation ranges of flood of HQ_{100} and flood of HQ_{50} are obtained. Then, Google Earth is used to get the towns and villages involved in inundation range (Figure 9). It can be seen that the impact of Gaobei Hydropower Project mainly involves five towns: Gaobei Twon, Yinjiang Twon, Dama Twon, Sanhe Twon, and Chayang Town in Dabu County. Besides, Gaobei Twon and Dama Twon are the most affected, followed by Yinjiang Town and Sanhe Town; Tea town is affected with the least land area.

It can be found that the differences of the inundation areas between the flood of HQ_{100} and flood of HQ_{50} are relatively small. There are large differences between A1 and A2 (Figure 10). The reason is that the topographical changes at most parts of inundation boundaries are relatively severe, that is to say, the slope of the mountain at the boundaries is steep. So the inundation range differences under different flood levels are small horizontally. In other words, the inundation ranges seems closed on the map. But, the topography at the inundation boundaries of some areas in A1 and A2 is relatively flat. So, the inundation ranges under different flood levels have a large difference in the horizontal direction. As a result, the two ranges appear to be different on the map. This phenomenon is in line with the geographical features of the Hanjiang River area. It proves the rationality of the analysis results.

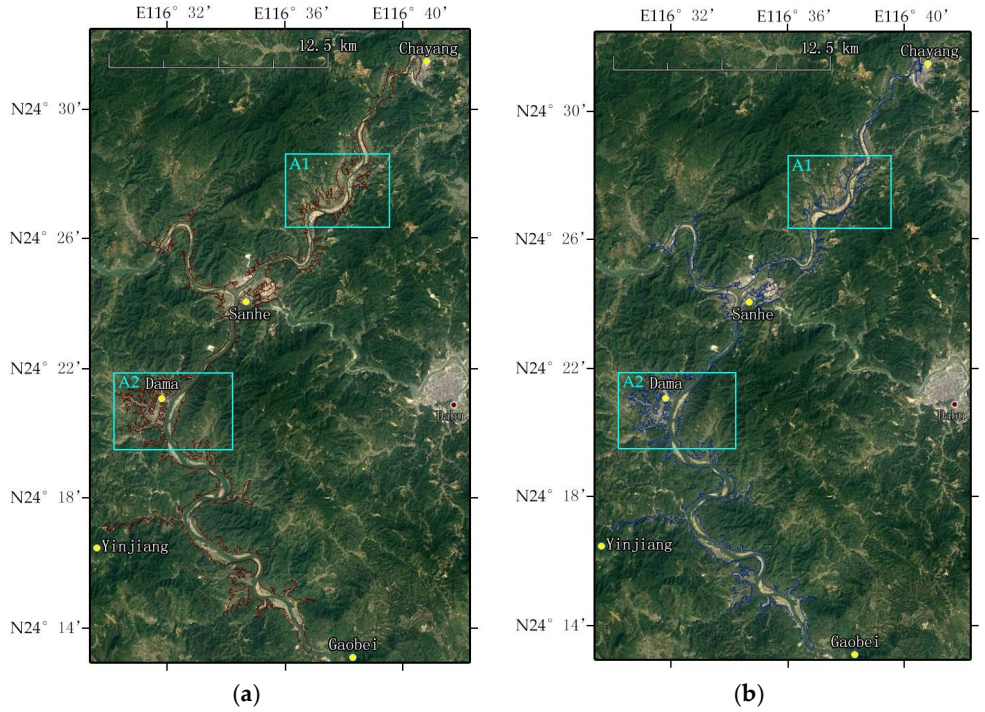

Figure 9. The flood inundation range of different return periods. (**a**) The flood inundation range of HQ_{100}; and, (**b**) The flood inundation range of HQ_{50}.

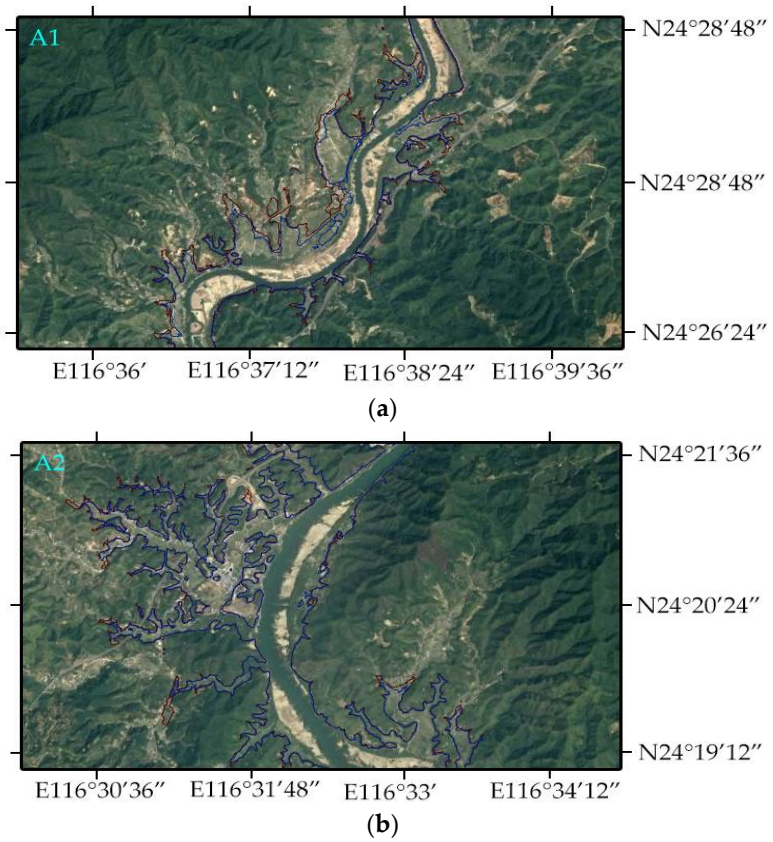

Figure 10. Inundation range of A1 and A2. (**a**) The inundation range difference in A1 section between HQ_{100} and HQ_{50} ; and, (**b**) The inundation range difference in A2 section between HQ_{100} and HQ_{50}.

4.2. Analysis of Inundation Depth of Study Area

For each sub-area, the raster calculator tool is used to calculate the inundation depth of each sub-area, according to the corresponding average backwater water level [39]. Combined with the DEM and the survey, the calculation results are corrected to obtain the flood inundation depth of HQ_{100} and HQ_{50}. Then, the different inundation depths are graded to obtain the schematic diagram of inundation depth (Figure 11). As can be seen from the figure, the inundation depth of the two banks of the river is between 0 m and 14 m, and the inundation depth shows a decreasing trend along the upstream of the river.

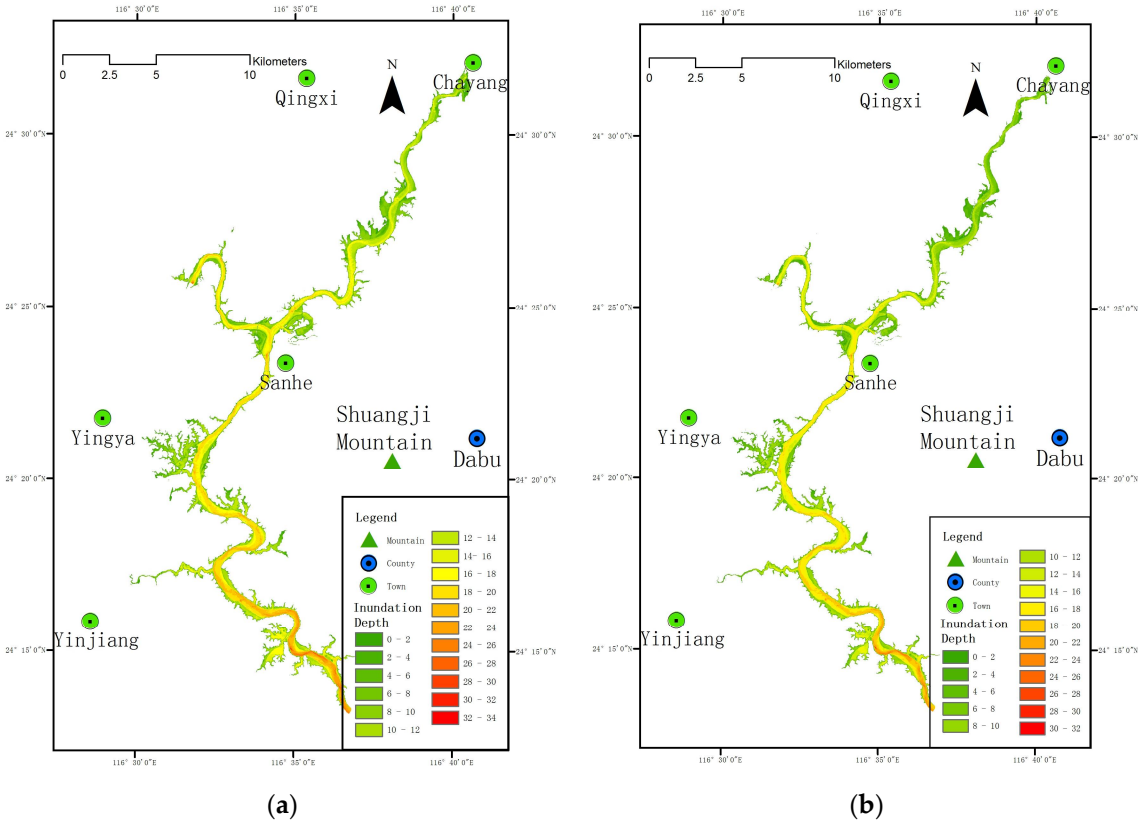

Figure 11. The flood inundation depth of different return periods. (**a**) The flood inundation depth of HQ_{100}; and, (**b**) The flood inundation depth of HQ_{50}.

4.3. Analysis of Inundation Area of Study Area

Inundation loss calculation requires inundation depth and area data. According to the above method, the resident migration range can be obtained. Based on the previously inundated raster file, the area that is covered by the migration range is removed. The depth and area of the inundation are calculated. Using the "Reclassify" tool to get the inundation area corresponding to inundation depth of 0–0.5 m, 0.5–1 m, 1–2 m, 2–4 m, and >4 m, as shown in Figure 12 [40]. It can be seen that the inundation area increases with the increase of inundation depth. Besides, the inundation area less than 4 m in flood of HQ_{50} is larger than the corresponding inundation area in the flood of HQ_{100}, but the difference is small. The situation is opposite when the inundation depth is greater than 4 m, and the difference is large. The difference reflects that, the larger the flood, the more the economic loss of the flood.

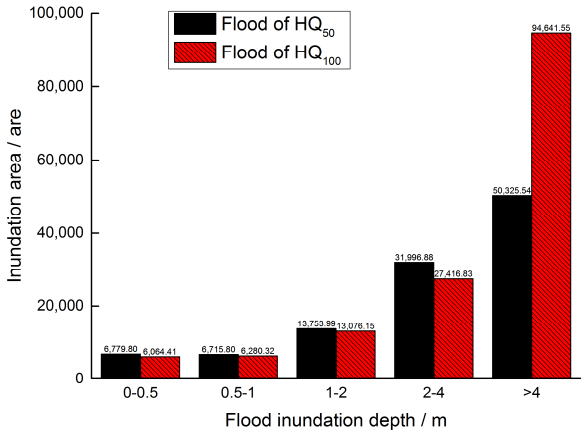

Figure 12. Flood inundation area of different return periods.

The topography of the river bank in one side can be generalized, as shown in the Figure 13. The length of line at different elevation represents the proportion of ground in different elevations. There can be two shapes, line A (pink line, blue line, green line, and yellow line) and line B (pink line, blue line, green line, and read line). For line A, it can be considered that the topographic changes at the inundation boundary are severe. The flood inundation ranges of HQ_{100} can be described with pink line + blue line + green line + yellow line. The flood inundation ranges of HQ_{50} can be expressed as pink line + blue line + green line. It can be seen that there is a small difference between the two ranges, which is shown with the yellow line. The flood inundation ranges with an inundation depth of less than 4 m of HQ_{100} can be described with green line + yellow line. The flood inundation ranges with inundation depth less than 4 m of HQ_{50} can be expressed as blue line + green line. It can be seen that the difference between the two ranges is the blue line − yellow line. In the case, the inundation areas of HQ50 with inundation depth less than 4 m are larger than that of HQ_{100}. For line B, it can be assumed that the topography at the inundation boundary is more gradual. The flood inundation ranges of HQ_{100} can be expressed as pink line + blue line + green line + red line. The flood inundation ranges of HQ_{50} can be expressed as pink line + blue line + green line. The flood inundation ranges with inundation depth less than 4 m of HQ_{100} can be expressed as green line + red line. The flood inundation ranges with an inundation depth of less than 4 m of HQ_{50} can be expressed as blue line + green line. It can be seen that the difference between the two ranges is the red line − blue line. It can be seen that the difference between the two ranges is red line − blue line. In this case, the inundation areas of HQ_{50} with inundation depth less than 4 m are smaller than that of HQ_{100}. According to the analysis above, most of the submerged boundaries belong to case line A, and the minority belongs to case line B. Therefore, for the entire inundation area, the inundation area of HQ_{50} with an inundation depth of less than 4 m is larger than that of HQ_{100}. Absolutely, the inundation area of HQ_{50} with inundation depth more than 4 m is smaller than that of HQ_{100}, for case line A and case line B.

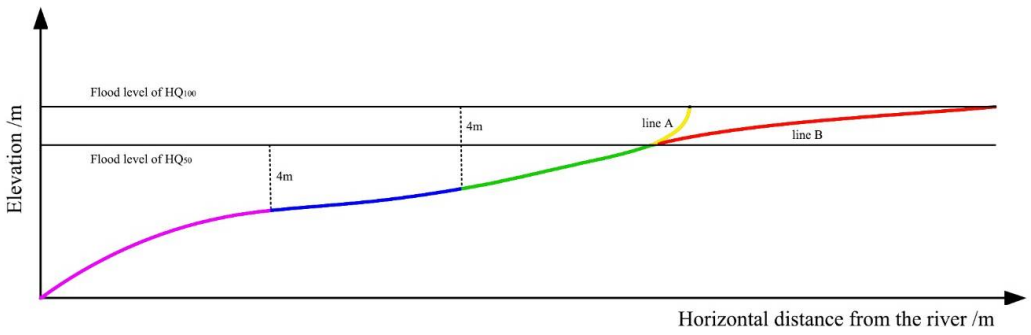

Figure 13. Schematic diagram of the topography of the river bank in one side.

4.4. Analysis of Inundation Loss in Study Area

When the reservoir encounters the rare flood or an extreme large flood, it will cause certain inundation losses to the reservoir area. The losses include the loss of property of residents and the loss of various special facilities. Our 15-person team spent two weeks investigating the study area. We counted the major physical indicators in the study area. According to the statistics, the major physical indicators that were affected by the flood inundation of HQ_{50} involve 25,023 registered residents, 861,619 m^2 of houses, and 58,880 ares of cultivated land. The main physical indicators of flood inundation of HQ_{100} involve 36,489 registered residents, 1,256,429 m^2 of houses, and 77,020 ares of cultivated land. Special facilities, roads, transformers, transmission lines, communication lines, cultural relics, and schools will all be affected by flooding, such as secondary roads, tertiary roads, and townships, 35 kV and 10 kV low-voltage distribution lines, China Mobile, China Unicom, China Telecom, and Meizhou local network lines. What's more, about 1% to 2% of the transformers in the area will be affected when the extreme large flood occurs.

According to the inundation range on the map, the inundation depth can be calculated according to the flood level and the local elevation. According to the proportion of inundation area under different water depths, the number of physical indicators that are inundated in different depths of water can be calculated. Based on the inundation water depths of floods at different return periods, the inundation time can be calculated to determine the inundation loss rate of different physical indicators. The loss of flood can be calculated based on the above data. According to the losses of family property and special facilities, it can be seen that the flood losses are 392.32 million RMB in flood of HQ_{50} and 610.02 million RMB in flood of HQ_{100}. At the same time, because the impact of floods involves the Zhongshan Park in Sanhe Town, Tianjiabing ancestral home of Tian Jiabing (an entrepreneur and philanthropist in Hong Kong), former residence of Lee Kuan Yew (the first prime minister of Singapore), and other cultural relics units, floods will damage the cultural relics and precious collections.

The above physical indicators and other indicators obtained from Hanjiang Gaobei Hydropower Project Preliminary Design Report are summarized in Table 1. As can be seen from the table, the results differences between the study and the report is small, so the analysis is reasonable. When compared with the physical indicators and the economic losses that are involved in normal pool level (HQ_{30}), the physical indicators that are involved in flood of HQ_{50} and flood of HQ_{100} have obviously increased, and so have the economic losses. Therefore, it is necessary to put forward feasible measures that reduce the effect of flooding. The compensation plan for inundation and the guarantee mechanism should be considered to guard the legitimate rights and interests of the masses in the reservoir area, protect stable economic and social development in the reservoir area, and provide the basis for the promulgation and formulation of relevant policies in the future.

Table 1. The physical indicators and economic losses in floods of different return periods.

Flood	Population		Houses/m^2		Land/are		Economic Loss/Million RMB	
	This Study	The Report	This Study	The Report	This Study	The Report	This Study	The Report
HQ_{30}		3745		142,697		21,608		66.89
HQ_{50}	25,023	24,861	861,619	856,041	58,880	59,960	392.32	399.01
HQ_{100}	36,489	36,254	1,256,429	1,248,337	77,020	76,640	610.02	628.54

5. Conclusions

Based on the topographic maps of CAD in the Hanjiang area, this paper analyzes the flood inundation around the Gaobei reservoir area by GIS and calculates the flood inundation loss. The conclusions are as follows:

(1) CAD topographic map can provide geographical basis information; the results can be directly applied to the GIS after a certain format conversion. ArcGIS platform enables the conversion of CAD data to GIS data. As long as the supplied CAD data is correct and meets the requirements, the ArcGIS platform can concert the CAD to DEM easily.

(2) It is feasible to use GIS software to analyze flood inundation. Based on the DEM data and the data of the backwater in the reservoir, the range of flood inundation, the flooded area, and the depth distribution of flooding can be simulated. Besides, the flooding loss can be calculated to provide a scientific basis for flood risk map and flood damage assessment. It provides support for government or management departments in guiding local residents to make rational arrangements for production and life and flood control decision-making.

Acknowledgments: This study was financially supported by National Key Research Projects "Water resources efficient development and utilization" (2017YFC0405900, 2016YFC0402208, and 2016YFC0401903) and National Natural Science Foundation of China (No. 51641901). We would like to express our sincere gratitude to editors and those anonymous reviewers.

Author Contributions: Jiqing Li and Jianchang Li conceived and designed the experiments; Jianchang Li and Kaiwen Yao performed the experiments; Jiqing Li and Kaiwen Yao analyzed the data; Kaiwen Yao contributed materials; Jiqing Li wrote the paper.

Conflicts of Interest: The authors declare no conflict of interest.

References

1. Chang, H.Y.; Shen, Y.F.; Wang, J.Y.; Huang, J.Y.; Lin, Y.T. Clustering-based hybrid inundation model for forecasting flood inundation depths. *J. Hydrol.* **2010**, *385*, 257–268. [CrossRef]
2. Sarhadi, A.; Soltani, S.; Modarres, R. Probabilistic flood inundation mapping of ungauged rivers: Linking GIS techniques and frequency analysis. *J. Hydrol.* **2012**. [CrossRef]
3. Sanders, B.F. Evaluation of on-line DEMs for flood inundation modeling. *Adv. Water Resour.* **2007**, *30*, 1831–1843. [CrossRef]
4. Srinivas, S.; Tripathi, A.R.; Rao, R.S. Govindaraju, Regional flood frequency analysis by combining self-organizing feature map and fuzzy clustering. *J. Hydrol.* **2008**, *348*, 148–166. [CrossRef]
5. Wu, L. Research on Flood Information System based on GIS and Database. Master's Thesis, Northwest University, Xi'an, China, 2005. (In Chinese)
6. Ding, Z.X.; Li, J.R.; Li, L. Method for flood submergence analysis based on GIS grid model. *J. Hydraul. Eng.* **2004**. (In Chinese) [CrossRef]
7. Ismail, E. Flash Flood Hazard Mapping Using Satellite Images and GIS Tools: A case study of Najran City, Kingdom of Saudi Arabia (KSA). *Egypt. J. Remote Sens. Space Sci.* **2015**, *18*, 261–278. [CrossRef]
8. Asare-Kyei, D.; Forkuor, G.; Venus, V. Modeling Flood Hazard Zones at the Sub-District Level with the Rational Model Integrated with GIS and Remote Sensing Approaches. *Water* **2015**, *7*, 3531–3564. [CrossRef]
9. Chen, J.; Arleen, A.H.; Lensyl, D.U. A GIS-based model for urban flood inundation. *J. Hydrol.* **2009**, *373*, 184–192. [CrossRef]
10. Zhang, S.H.; Pan, B.Z. An urban storm-inundation simulation method based on GIS. *J. Hydrol.* **2014**, *517*, 260–268. [CrossRef]
11. Ouma, Y.O.; Tateishi, R. Urban Flood Vulnerability and Risk Mapping Using Integrated Multi-Parametric AHP and GIS: Methodological Overview and Case Study Assessment. *Water* **2014**, *6*, 1515–1545. [CrossRef]
12. Gigovic, L.; Pamucar, D.; Bajic, Z.; Drobnjak, S. Application of GIS-Interval Rough AHP Methodology for Flood Hazard Mapping in Urban Areas. *Water* **2017**, *9*, 360. [CrossRef]
13. Lyu, H.-M.; Wang, G.-F.; Shen, J.S.; Lu, L.-H.; Wang, G.-Q. Analysis and GIS Mapping of Flooding Hazards on 10 May 2016, Guangzhou, China. *Water* **2016**, *8*, 447. [CrossRef]
14. Jato-Espino, D.; Sillanpää, N.; Charlesworth, S.M.; Andrés-Doménech, I. Coupling GIS with Stormwater Modelling for the Location Prioritization and Hydrological Simulation of Permeable Pavements in Urban Catchments. *Water* **2016**, *8*, 451. [CrossRef]
15. Townsend, P.A.; Walsh, S.J. Modeling floodplain inundation using an integrated GIS with radar and optical remote sensing. *Geomorphology* **1998**, *21*, 295–312. [CrossRef]

16. Avidesh, S.; Matthew, W.; Keith, M. Hydrodynamic versus GIS modelling for coastal flood vulnerability assessment: Which is better for guiding coastal management? *Ocean Coast. Manag.* **2016**, *120*, 99–109. [CrossRef]
17. Bhuyian, M.N.M.; Kalyanapu, A.; Hossain, F. Evaluating Conveyance-Based DEM Correction Technique on NED and SRTM DEMs for Flood Impact Assessment of the 2010 Cumberland River Flood. *Geosciences* **2017**, *7*, 132. [CrossRef]
18. Walczak, Z.; Sojka, M.; Wrózynski, R.; Laks, I. Estimation of Polder Retention Capacity Based on ASTER, SRTM and LIDAR DEMs: The Case of Majdany Polder (West Poland). *Water* **2016**, *8*, 230. [CrossRef]
19. Saksena, S.; Merwade, V. Incorporating the effect of DEM resolution and accuracy for improved flood inundation mapping. *J. Hydrol.* **2015**, *530*, 180–194. [CrossRef]
20. Van de Sande, B.; Lansen, J.; Hoyng, C. Sensitivity of Coastal Flood Risk Assessments to Digital Elevation Models. *Water* **2012**, *4*, 568–579. [CrossRef]
21. Heimhuber, V.; Hannemann, J.-C.; Rieger, W. Flood Risk Management in Remote and Impoverished Areas—A Case Study of Onaville, Haiti. *Water* **2015**, *7*, 3832–3860. [CrossRef]
22. Laks, I.; Sojka, M.; Walczak, Z.; Wrózynski, R. Possibilities of Using Low Quality Digital Elevation Models of Floodplains in Hydraulic Numerical Modelst. *Water* **2017**, *9*, 283. [CrossRef]
23. Javaheri, A.; Nabatian, M.; Omranian, E.; Babbar-Sebens, M.; Noh, S.J. Merging Real-Time Channel Sensor Networks with Continental-Scale Hydrologic Models: A Data Assimilation Approach for Improving Accuracy in Flood Depth Predictions. *Hydrology* **2018**, *5*, 9. [CrossRef]
24. National Park Service. CAD TO GIS: A Step-By-Step Guide to Converting .dwg CAD Files to GIS Shapefiles Using AutoCAD 2002 (AutoDesk) and ArcGIS 8.3 (ESRI). 2005. Available online: https://wenku.baidu.com/view/2e76501ca300a6c30c229f1b.html (accessed on 18 April 2018).
25. Rebecca, O.C.T.; Christopher, G. TIN meets CAD—Extending the TIN concept in GIS. *Future Gener. Comput. Syst.* **2004**, *20*, 1171–1184. [CrossRef]
26. Pu, S.; Zlatanova, S. Integration of GIS and CAD at DBMS Level. Available online: http://citeseerx.ist.psu.edu/viewdoc/download?doi=10.1.1.616.4496&rep=rep1&type=pdf (accessed on 18 April 2018).
27. Zlatanova, S.; Stoter, J. The role of DBMS in the new generation GIS architecture. In *Frontiers of Geographic Information Technology*; Rana, S., Sharma, J., Eds.; Springer: Berlin, Germany, 2006; pp. 155–180.
28. Ratchata, P.; Hassan, A.K.; Burcu, A.; Frank, B. An ontological engineering approach for integrating CAD and GIS in support of infrastructure management. *Adv. Eng. Inf.* **2006**, *20*, 71–88. [CrossRef]
29. Jelena, C. ArcGIS ModelBuilder functionality for CAD to GIS conversion using spatial ETL procedures. *Geonauka* **2013**. [CrossRef]
30. Wang, Q.G. Management of CAD Relief Map and Location of Project Based on GIS. Master's Thesis, China University of Geosciences, Beijing, China, 2006. (In Chinese)
31. He, X.P. The Analysis Method in Calculation of Reservoir Capacity. *J. Nanchang Coll. Water Conserv. Hydroel. Power* **1998**, *4*, 57–61. (In Chinese)
32. Doyle, F.J. Digital terrain models: An overview. *Photogram. Eng. Remote Sens.* **1978**, *44*, 1481–1485.
33. Liu, R.Y.; Liu, N. A GIS Based Model for Calculating of Flood Area. *Acta Geogr. Sin.* **2001**, *56*, 1–6. (In Chinese) [CrossRef]
34. Liu, R.Y.; Liu, N. A New DEM-based Method for Flood Area Calculation and Damage Evaluation. *J. Image Graph.* **2001**. (In Chinese) [CrossRef]
35. Guo, L.H.; Long, Y. Analysis of Flood Submerging Based on DEM. *Bull. Surv. Map.* **2002**. (In Chinese) [CrossRef]
36. Liu, X.S.; Chen, Y.J.; Huang, Y.S. The ascertainment of flood area based on GIS. *Sci. Surv. Map.* **2007**. (In Chinese) [CrossRef]
37. Zhang, D.H.; Liu, R.; Zhang, Y.X.; Xie, J.H. The Design and Implement of a New Algorithm to Calculate Source Flood Submerge Area Based on DEM. *J. East Chin. Inst. Technol. (Nat. Sci.)* **2009**, *2*, 181–184. (In Chinese)
38. Song, G.F.; Zhong, E.S. Research and Development of Components Geographic Information Systems. *J. Image Graph.* **1998**, *3*, 313–317. (In Chinese)

39. Yang, Q.; Jia, A.C. Research on Inundation Area of Flood Disaster and Evacuation Plan Based on ArcGIS. *Water Resour. Power* **2011**, *29*, 35–36. (In Chinese)
40. Sun, A.L.; Xu, L.S.; Shi, Y.; Shi, C. Flood Submerged Area Simulation Based on GIS. *J. North Chin. Inst. Water Conserv. Hydroel. Power* **2009**, *30*, 9–11. (In Chinese) [CrossRef]